1. General

Alloy 22-13-5 is a nitrogen-strengthened austenitic stainless steel with good mechanical properties and excellent corrosion resistance at room temperature and cryogenic temperatures. Yield strengths greater than 1000 MPa can be achieved in this alloy by warm-working. Although ferrite is typically not observed in bar stock, solidification of primary ferrite is thought to be important for high quality fusion welds and may then be observed in welded joints.

Although very little data exist for 22-13-5 in gaseous hydrogen environments, published data indicate that this alloy is not strongly affected by hydrogen gas environments even at cryogenic temperatures. This is attributed to the relatively high stacking fault energy in this alloy [1, 2], which promotes cross slip.

1.1 Composition

Table 1.1.1 lists the composition ranges specified in two standards for 22-13-5 and the compositions of several heats of 22-13-5 used to study hydrogen effects.

1.2 Other Designations

Nitronic 50, XM-19, UNS S20910

2. Permeability and Solubility

No known published data. Ref. [5] provides a summary of data for other stainless steels.

3. Mechanical Properties in the Presence of Internal and External Hydrogen

3.1 Tensile properties

3.1.1. Smooth tensile properties

Basic tensile properties of hydrogen-exposed 22-13-5 from a number of studies at room temperature are summarized in Table 3.1.1.1. Figure 3.1.1.1 shows the effects of both internal and external sources of hydrogen on the tensile properties of two forgings [3]. The effect of temperature is shown in Figure 3.1.1.2 for 22-13-5 thermally charged with hydrogen [6]. For the conditions explored in these studies, 22-13-5 shows little if any degradation of tensile ductility. In some cases, hydrogen appears to increase yield stress, although this effect is small.

3.1.2 Notched tensile properties

The reduction of area measured in notched tensile specimens is shown in Fig. 3.1.2.1 for two heats of 22-13-5 subjected to two heat treatments in the uncharged and thermally hydrogen charged conditions. These materials show a relatively modest loss of ductility due to hydrogen. These data also demonstrate the importance of microstructural control as the loss in ductility due to thermal exposure at 800˚C is greater than the loss due to hydrogen exposure in material heat treated at 1000˚C, see section 4.2.

3.2 Fracture mechanics

3.2.1 Fracture toughness

No known published data.

3.2.2 Threshold stress intensity

No crack propagation was observed in Wedge-Open Loading (WOL) testing in hydrogen gas at a stress intensity of 132 MPa $m^{1/2}$ [7]. The material, P81 Table 1.1.1, was high energy rate forged at 980˚C, and had a yield strength of 724 MPa. The WOL specimen was loaded in 200 MPa hydrogen gas at ambient temperature for 5000 hours. The testing procedure is believed to have satisfied the requirements of ASTM E 1681-99 [8].

3.3 Fatigue

No known published data.

3.4 Creep

No known published data.

4. Fabrication

4.1 Primary processing

4. 2 Heat treatment

Control of processing temperatures is important, as there is some evidence that brittle second phases can form at temperatures less than 850˚C [2] (also refer to trends in data from Ref. [3]). In similar alloys such as 21-6-9, ferrite may rapidly transform to brittle σ-phase in the temperature range of about 650˚C to 900˚C [4]. These microstructural issues are independent of hydrogen exposure, but could exacerbate hydrogen-assisted fracture.

4.3 Properties of welds

Detailed microstructural investigation of 22-13-5 GTA (gas tungsten arc) welds in hydrogen are presented in Ref. [9, 10]. The base material for these studies was HERF (high energy rate forging), back extrusions of 22-13-5, machined to cylindrical shape (10 cm diameter, 1.5 cm wall thickness) with circumferential double J grooves. The filler material was also 22-13-5 matched to the composition of the base metal. The composition of the weld fusion zone is given in Table 1.1.1. Tensile specimens were machined with the weld zone centered in the gauge section, and in all cases the composite gauge section (weld fusion zone, heat affected zone and base material) fractured within the weld. Fracture of the welds was by microvoid coalescence (dimple rupture) and hydrogen exposure did not significantly alter the morphology of the fracture surfaces. The tensile properties are listed in Table 4.1.1. These data are shown for reference only as they represent the properties of a composite specimen, however, they do demonstrate the effect of hydrogen on the ductility of the welds.

5. References

1. BC Odegard, JA Brooks and AJ West. The Effect of Hydrogen on Mechanical Behavior of Nitrogen-Strengthened Stainless Steel. in: AW Thompson and IM Bernstein, editors. Effect of Hydrogen on Behavior of Materials. New York: TMS (1976) p. 116-125.
2. BP Somerday and SL Robinson. H- and Tritium-Assisted Fracture in N-Strengthened, Austentitic Stainless Steel. J Metals 55 (2003) 51-55.

3. BC Odegard and AJ West. On the Thermo-Mechanical Behavior and Hydrogen Compatibility of 22-13-5 Stainless Steel. Mater Sci Eng 19 (1975) 261-270.
4. CL Ferrera. The Formation and Effects of Sigma Phase in 21-6-9 Stainless Steel. PMT-87-0017, Rockwell International, Rocky Flats Plant, Golden CO (November 1987).
5. GR Caskey. Hydrogen Effects in Stainless Steels. in: RA Oriani, JP Hirth and M Smialowski, editors. Hydrogen Degradation of Ferrous Alloys. Park Ridge NJ: Noyes Publications (1985) p. 822-862.
6. GR Caskey. Hydrogen Damage in Stainless Steel. in: MR Louthan, RP McNitt and RD Sisson, editors. Environmental Degradation of Engineering Materials in Hydrogen. Blacksburg VA: Laboratory for the Study of Environmental Degradation of Engineering Materials, Virginia Polytechnic Institute (1981) p. 283-302.
7. MW Perra. Sustained-Load Cracking of Austenitic Steels in Gaseous Hydrogen. in: MR Louthan, RP McNitt and RD Sisson, editors. Environmental Degradation of Engineering Materials in Hydrogen. Blacksburg VA: Laboratory for the Study of Environmental Degradation of Engineering Materials, Virginia Polytechnic Institute (1981) p. 321-333.
8. ASTM E 1681-99, Standard Test Method for Determining Threshold Stress Intensity Factor for Environment-Assisted Cracking of Metallic Materials. American Society for Testing and Materials (1999).
9. JA Brooks and AJ West. Hydrogen Induced Ductility Losses in Austenitic Stainless Steel Welds. Metall Trans 12A (1981) 213-223.
10. JA Brooks, AJ West and AW Thompson. Effect of Weld Composition and Microstructure on Hydrogen Assisted Fracture of Austenitic Stainless Steels. Metall Trans 14A (1983) 75-84.
11. AMS 5764E, Steel, Corrosion-Resistant, Bars, Wire, Forgings, Extrusions and Rings 5.0Mn-22Cr-12.5Ni-2.2Mo-0.20Cb-0.30N-0.20V Solution Heat Treated. Society of Automotive Engineers (2003).
12. ASTM F 1314-01, Standard Specification for Wrought Nitrogen Strengthened 22 Chromium - 13 Nickel - 5 Manganese - 2.5 Molybdenum Stainless Steel Alloy Bar and Wire for Surgical Implants (UNS S20910). American Society for Testing and Materials (2001).
13. GR Caskey. Hydrogen Compatibility Handbook for Stainless Steels. DP-1643, EI du Pont Nemours, Savannah River Laboratory, Aiken SC (June 1983).
14. TL Capeletti and MR Louthan. The Tensile Ductility of Austenitic Steels in Air and Hydrogen. J Eng Mater Technol 99 (1977) 153-158.

Table 1.1.1. Composition of several heats of 22-13-5 used to study hydrogen effects as well as specification limits.

heat	Cr	Ni	Mn	Mo	Si	C	N		Ref.
AMS 5764E	20.50 23.50	11.50 13.50	4.00 6.00	1.50 3.00	1.00 max	0.06 max	0.20 0.40	0.030 max S; 0.040 max P	[11]
ASTM F1314	20.50 23.50	11.50 13.50	4.00 6.00	2.00 3.00	0.75 max	0.030 max	0.20 0.40	0.10 max S; 0.025 max P	[12]
O75	22.15	12.74	5.26	2.20	0.50	0.050	0.34	0.006 S; 0.019 P; 0.23 Nb; 0.26 V	[3]
O76	23.00	12.98	4.68	1.75	0.36	0.050	0.38		[1]
P81	23.11	12.91	4.76	1.75	0.38	0.05	0.39	0.18 Nb	[7]
C83	21.48	12.36	5.44	2.12	0.42	0.05	0.25	0.010 S; 0.015 P; 0.19 Nb; 0.2 V	[13]
B83*	22.9	12.9	4.6	1.8	0.42	0.05	0.35	0.008S; 0.012 P	[10]
S03a	21.26	11.87	4.67	2.20	---	0.036	0.276		[2]
S03b	21.32	13.11	5.02	2.04	---	0.013	0.30		[2]

* composition in GTA weld fusion zone

Table 3.1.1.1. Tensile properties of 22-13-5 exposed to and tested in hydrogen gas at room temperature.

Material	Test environment	Thermal precharging	S_y (MPa)	S_u (MPa)	El_u (%)	El_t (%)	RA (%)	Ref.
Bar, as-received, heat C83	Air	None	440	710	---	43	72	[6, 13, 14]
	69MPa He	None	400	680	---	47	74	
	69MPa H_2	None	400	680	---	45	73	
Bar, as-received	Air	None	800*	1190†	32	41	69	[13]
	Air	(1)	820*	1240†	33	44	65	
Annealed plate, heat O76	Air	None	586	938	---	51	67	[1]
	69MPa H_2	(2)	579	951	---	54	68	
Warm-worked bar, heat O75	Air	None	841	958	30	---	66	[3]
	69MPa H_2	None	841	986	27	---	67	
	Air	(2)	855	1007	27	---	64	
	69MPa H_2	(2)	924	1082	23	---	62	
HERF, heat O75	Air	None	1269	1317	9	---	20	[3]
	69MPa H_2	None	1202	1276	7	---	29.5	
	Air	(2)	1262	1310	10	---	15.5	
	69MPa H_2	(2)	1310	1365	10	---	20	

(1) 69MPa hydrogen gas, 620K, 3 weeks
(2) 24MPa hydrogen gas, 473K, 10.5 days: calculated surface concentration of ~50 wppm hydrogen (~2500 appm)
* true stress at 5% strain
† true stress at maximum load

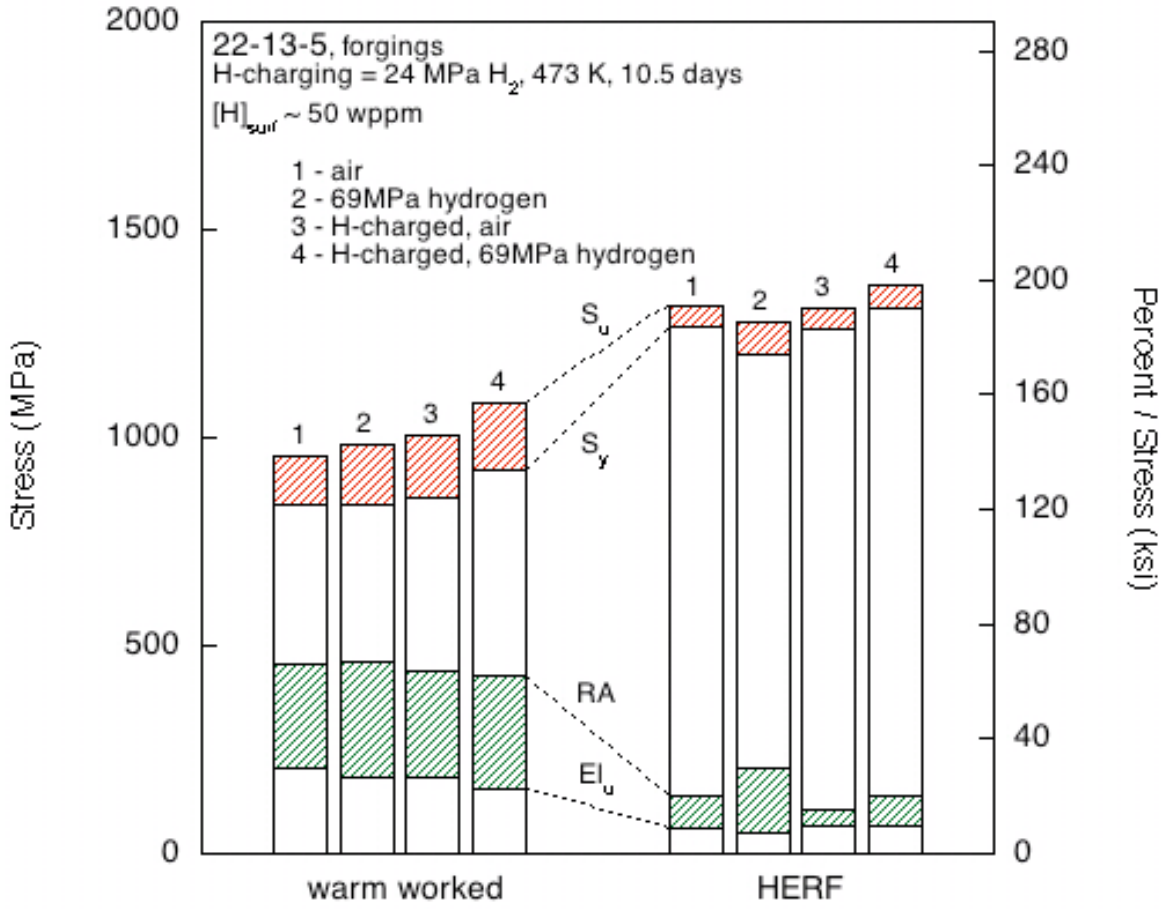

Figure 3.1.1.1. Effect of internal and external hydrogen on the tensile properties of 22-13-5 forgings (heat O75) from Ref. [3]; same data is contained in Table 3.1.1.1. Strain rate of tensile testing was 3×10^{-4} s^{-1}. (HERF = high energy rate forging)

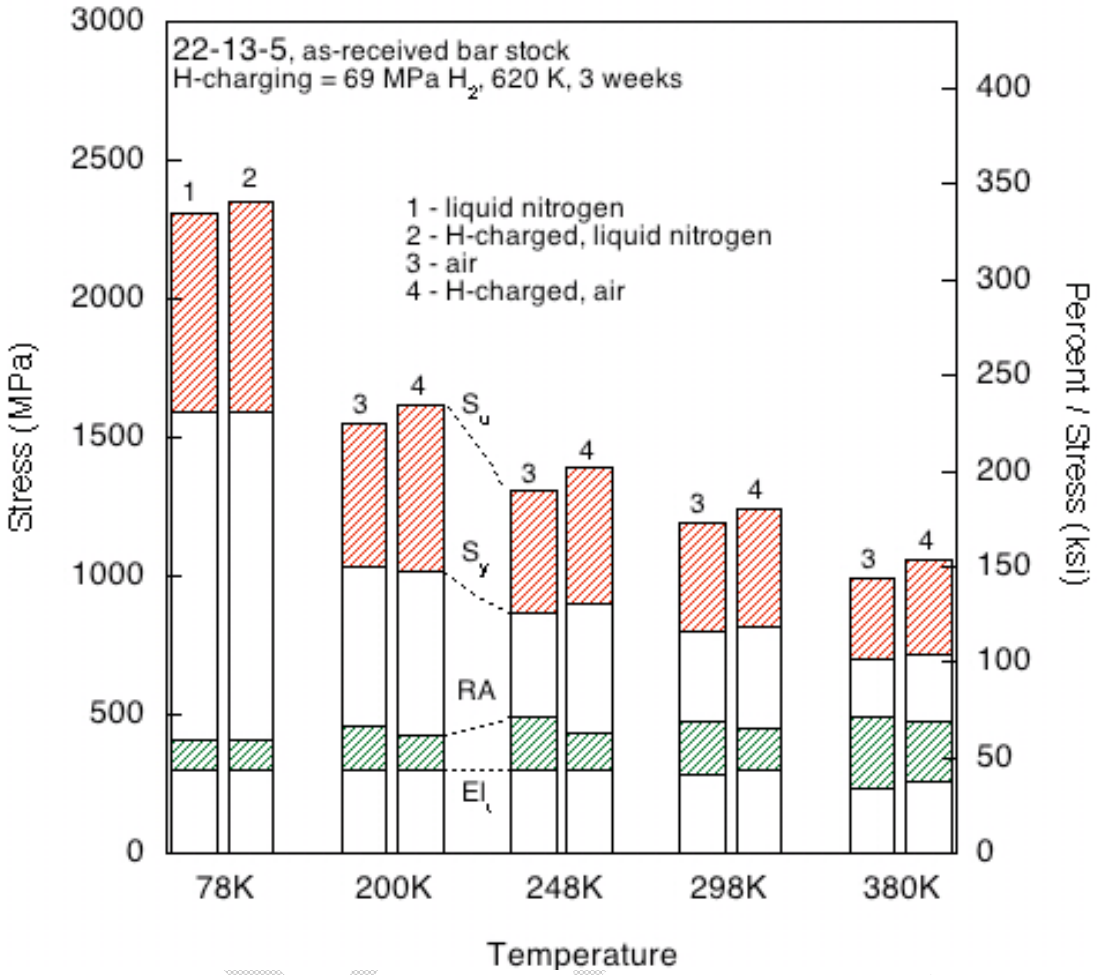

Figure 3.1.1.2. Effect of temperature on the hydrogen compatibility of 22-13-5 bar stock from Ref.[13]. Yield strength in this plot is defined as the true stress at 5% strain.

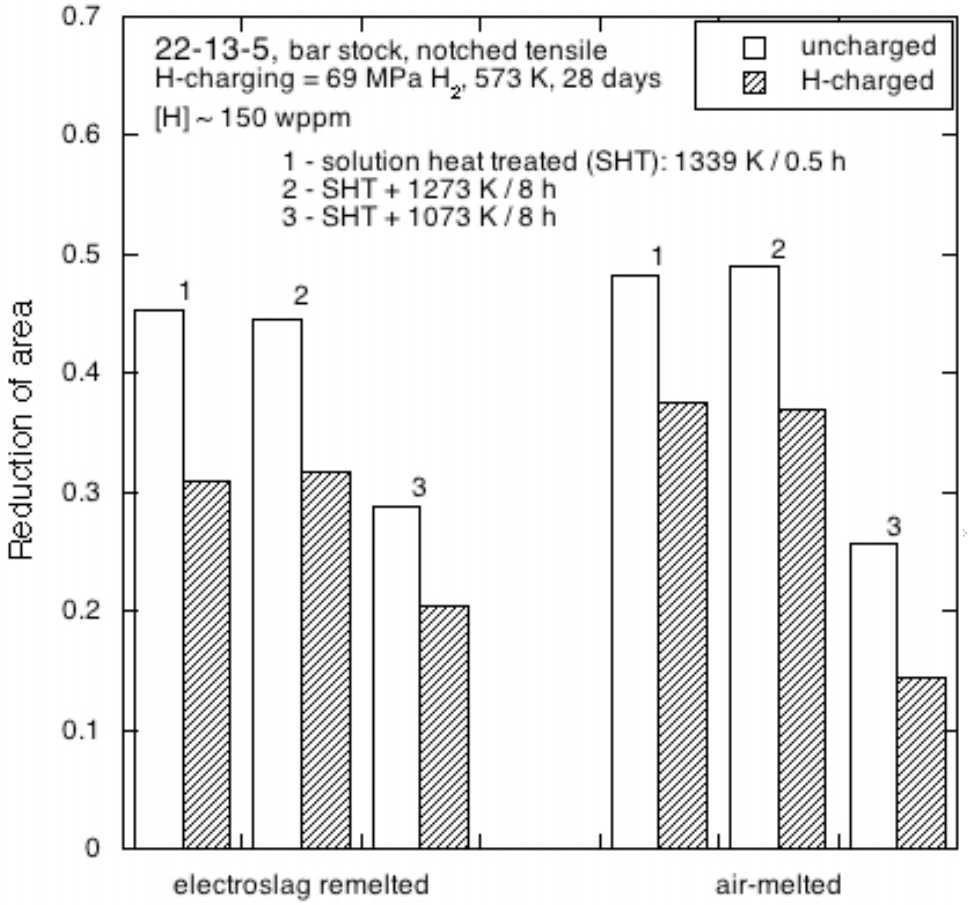

Figure 3.1.2.1. Notched tensile tests of two heats of 22-13-5 (electroslag remelted S03b; air-melted S03a) from Ref. [2]. The minimum and maximum diameters of the specimens were 3.9 and 7.9□mm respectively with a semicircular notch profile of 0.79□mm radius. Specimens were tested at a constant rate of displacement of 6×10^{-3} mm/s.

Table 4.1.1. Tensile properties of 22-13-5 composite GTA weld specimens (contains base material and heat affected zone with the fusion zone centered in the gauge length) exposed to and tested in hydrogen gas at room temperature [10]. All data are provided for completeness, but it should be emphasized that these values may not reflect the properties of any of the specific microstructures within the gauge length. Strain rate = 3.3×10^{-4} s^{-1}

Test environment	Thermal precharging	S_y (MPa)	S_u (MPa)	El_u (%)	El_t (%)	RA (%)
Air	None	495	782	11.2	14.4	49
69MPa H_2	None	511	778	13.0	16.3	48
172MPa H_2	None	528	798	11.8	16.0	50
Air	24MPa H_2 473K, 10 days*	510	789	9.6	10.9	38
69MPa H_2		531	776	10.2	12.0	45
Air	69MPa H_2 473K, 10 days*	514	789	9.9	10.7	35
172MPa H_2		516	780	11.6	13.5	35

* Hydrogen concentration was predicted to vary from the surface to the center of the specimens and was estimated to be 50 to 4 wppm (2500 to 200□ppm) surface to center for the low pressure charging condition (24 MPa) and 75 to 7 wppm (4000 to 400□ppm) for the high pressure charging condition (69 MPa).